STRESS FIELD AND FORMATION OF FRACTURE NETWORK IN THE SOLIDIFIED MAGMA REGION FOR THE DIRECT UTILIZATION OF MAGMA ENERGY

Kazuo HAYASHI[1], Kiyoshi TAKEUCHI[2] and Hiroyuki ABÉ[3]

(1) Institute of Fluid Science, Tohoku University, Sendai 980, Japan
(2) Sekisui Chemi. Co. Ltd., Wadai 32, Tsukuba 300-42, Japan
(3) Faculty of Engineering, Tohoku University, Sendai 980, Japan

key words: magma energy, open system, stress field, fracture network

ABSTRACT

In the extraction of thermal energy from magma, it is expected that a fracture network would be created due to thermal contraction of the solidified magma formed around the wellbore during heat extraction and the fracture network is expected to work as the flow path of the working fluid for the heat extraction. In the present paper, the stress field in the solidified magma and its variation with respect to time were analyzed based on the creep theory, emphasizing the feasibility of formation of the fracture network for a various types of rocks.

1. INTRODUCTION

The basic concept of extracting heat directly from molten magma was proposed by Sandia National Laboratories in the beginning of the 1970's. Since then, magma energy has attracted intensive attentions as one of the most potential candidates of renewable and sustainable natural energy sources and extensive efforts have been made to clarify scientific and engineering feasibilities of the direct heat extraction from magma (Colp and Stoller, 1981; Gerlach, 1981; Colp, 1982; Dunn, 1989; Chu et al., 1990). Two types have been proposed for the direct heat extraction system created in molten magma, i.e., closed and open systems. The closed system consists of concentric tubes set in magma which essentially form a counter flow heat exchanger. Water is pumped down through the outer annuls, extracts heat and goes back to the surface through the insulated inner tube. In the open system, water is pumped down through an insulated tube set in magma. It is envisaged that fractures due to thermal contraction are created around the tube in the solidified region formed in the molten magma. The water goes out from the lower end of the tube into the fractures and extracts heat by direct contact with the solidified magma. The heated water is retrieved near the upper part of magma and flows back to the surface.

The solidified region formed around the tube supports the high confining pressure which can be several hundred megapascals for a system of 10km deep. Furthermore, fractures in the solidified magma serves as flow paths of heated water in the case of the open system. Therefore, the stability of the solidified region is one of the crucial problems in the direct heat extraction from molten magma. So far, attentions have been focused mostly to the problems relating to the heat transfer of the heat extract systems, where the process of solidification of magma due to heat extraction is discussed in a rough approximation by giving the heat flux at the outer boundary of the solidified region (Hicox and Dunn, 1985; Dunn et al., 1987; Boehm et al., 1989). Also rather extensive efforts have been exerted to the problems of material compatibility between magma and metals (Westrich et al., 1986). However, regarding the problems of stability of solidified region, our knowledge is very restricted. Only the stress field obtained by thermoelasticity (Dunn, 1983) and results of lab-experiments simulating formation of fractures without confining pressure (Dunn et al., 1987; Chu et al., 1990) are available.

In the previous paper we analyzed the problem of heat transfer to obtain the temperature field, where the existence of mushy region in between the solidified and molten magma was taken into account, and processes of growth and remelting of the solidified region were studies in detail (Hayashi et al., 1991). In the present paper, by utilizing the temperature field obtained in the previous paper, the stress field in the solidified magma and its variation with respect to time were analyzed for the open system based on the creep theory, emphasizing the feasibility of formation of the fracture network for a various type of rocks, i.e., granite, olivine and anorthosite. As for the constitutive law for the creep, the usual incremental flow theory is employed, where the second invariant of the stress deviator is used as the creep potential.

2. OPEN SYSTEM AND MODEL FOR STRESS ANALYSIS

Figure 1 illustrates the open system schematically. The system is usually several kilometers deep. Around the wellbore there exists solidified magma and outermost region is molten magma. Partially solidified magma occupies the region in between the two regions. The solidified magma supports the high confining pressure as high as several megapascals against collapse of the wellbore. The size of the solidified region in the horizontal plane is expected to be 100 times as large as the wellbore radius at most, whereas the vertical length of the heat exchange system is expected to be more than 1000m (Dunn et al., 1987; Hayashi, 1991). Therefore the heat exchange system is very slender in the vertical direction. Thus, as a first approximation, stress state is assumed to be under the plane strain condition parallel to the horizontal plane, except for the upper and lower parts of the heat exchange system. In the following, the stress field is discussed in the horizontal plane, restricting our attentions to the intermediate part of the heat exchange system (Figure 2).

3. STRESS ANALYSIS

Let us introduce a Cartesian coordinate system (x_1, x_2, x_3) and a polar coordinate system (r, θ, z) centered at the center of the wellbore (Figure 2). The stress and strain are denoted as σ_{ij} and ϵ_{ij} referred to the Cartesian coordinate system, respectively. It is readily understood that the deformation is axisymmetric. The

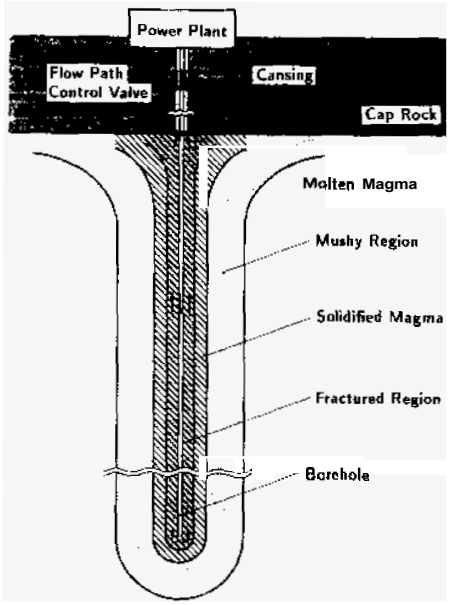

Figure 1. Open system for heat extraction from magma

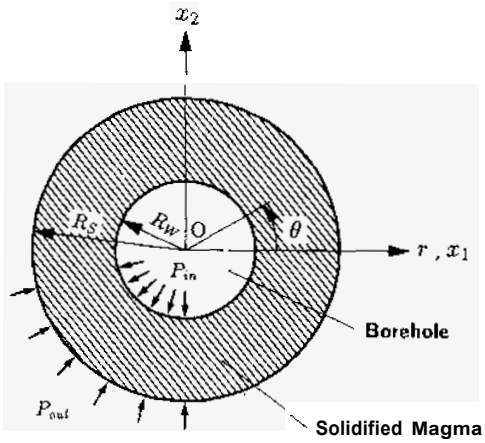

Figure 2. Geometry of solidified region and the coordinate systems.

strain consists of three terms as follows:

$$\epsilon_{ij} = \epsilon^e_{ij} + \delta_{ij}\int_{T_0}^{T} \alpha dT + \epsilon^c_{ij} \tag{1}$$

where T is temperature, T_0 the temperature of zero strain, α coefficient of thermal expansion and δ_{ij} Kronecker delta. The strains ϵ^e_{ij} and ϵ^c_{ij} denote the elastic and creep strains, respectively. By using eq. (1), the equation of equilibrium, the equation of compatibility and the Hooke's low for elastic strains, we finally arrive at the following differential equation:

$$r\frac{d^2\sigma_r}{dr^2} + 3\frac{d\sigma_r}{dr} = \frac{E}{1-\nu^2}\left[\frac{\epsilon^c_r - \epsilon^c_\theta}{r} - \frac{d}{dr}\left\{(1+\nu)\int_{T_0}^{T}\alpha dT + \epsilon^c_\theta + \nu\epsilon^c_z\right\}\right] \tag{2}$$

where E and ν are Young's modulus and Poisson's ratio, respectively. The differential equation is accompanied by the following boundary condition:

$$\sigma_r(R_w) = -P_{in}, \qquad \sigma_r(R_s) = -P_{out} \tag{3}$$

where P_{in} and P_{out} are the normal stresses acting normally to the inner and outer boundaries of the solidified region. Let us employ the following uniaxial stress-strain relation for the creep deformation:

$$\dot{\epsilon}^c = A t \sigma^m \exp\left(-\frac{\Delta H}{RT}\right) \tag{4}$$

where A and m are material constants, ΔH activation energy, R Boltzmann constant and T absolute temperature. Then the so-called J_2 flow theory leads us to the following constitutive law:

$$\dot{\epsilon}^c_{ij} = \frac{3}{2}\frac{\dot{\epsilon}_e}{\sigma_e}s_{ij} \tag{5}$$

where s_{ij} is stress deviator. The effective stress σ_e and effective strain rate $\dot{\epsilon}_e$ are defined by

$$\sigma_e = \sum_{i,j=1}^{3}\left(\frac{3}{2}s_{ij}s_{ij}\right)^{1/} \tag{6}$$

$$\dot{\epsilon}_e = \sum_{i,j=1}^{3}\left(\frac{2}{3}\dot{\epsilon}^c_{ij}\dot{\epsilon}^c_{ij}\right)^{1/2} \tag{7}$$

The symbol ($\dot{}$) denotes the derivative with respect to time, i.e. $\dot{\epsilon}^c_{ij}$ is the creep strain rate. The total creep strain is obtained by integrating the strain rate along the loading path.

4. STRESS STATE AND FORMATION OF FHACTUHE NETWORK

The problem defined by eqs.(2)-(7) is nonlinear. The so-called method of successive elastic solutions (Mendelson, 1986) is employed to solve the problem, and the stresses are calculated step by step with a small time step starting from the situation of $R_s/R_w = 1.5$ which corresponds to $t \cong 0.1$hr approximately after the onset of heat extraction. The temperature field is determined following the previons paper (Hayashi et al., 1991). The temperature profiles for several representative times after the onset of heat extraction are shown in Appendix. Following values are used:

$$R = 8.3J/(\mathrm{mol}\cdot K),\ E = 50\mathrm{GPa},$$
$$\alpha = 9\times 10^{-6}K^{-1},\ \nu = 0.25$$

At the temperature of solidus, solidified magma is assumed to be stress free. The temperature of solidus is set to be 800°C for granite and anorthosite and 1000°C for olivine, whereas as to the coefficient of thermal expansion, Young's modulus and Poisson's ratio the identical valuse listed above are used for the three types of rock referring to Dunn (1983). Pressures at the inner and outer boundaries are set to be 100MPa and 250MPa, respectively supposing 10km deep, unless otherwise stated. As to the material constants A, m and ΔH, the values presented in Table 1 are used (Kirby and Kronenberg, 1987). Table 2 summarizes the creep strain rates for the uni-axial stress condition of $\sigma = 500$MPa under $T = 600$°C. As can be seen from Table 2, granite deforms by creep most easily among the three and olivine is most resistive to creep. Anorthosite has intermediate characteristic. As stated before, the plane strain condition parallel to the horizontal plane is assumed. However, overburden pressure is also acting in the vertical direction. The normal stress in the vertical direction presented in the following figures is the sum of the overburden pressure and the stress ob-

Table 1. Creep properties of rocks.

Rock	$\log_{10}A$ $\mathrm{MPa}^{-m}\cdot\mathrm{s}^{-1}$	m	ΔH $\mathrm{kJ}\cdot\mathrm{mol}^{-1}$
Granite	3.7	1.9	137
Olivine	4.0	3.4	444
Anorthosite	-3.7	3.2	238

Table 2 Characteristics of creep deformation of rucks under a representative condition (uni-axial deformation, $\sigma = 500$MPa, $T = 600$°C).

Rock	Creep Strain Rate s^{-1}
Granite	1.97×10^{-7}
Olivine	5.07×10^{-14}
Anorthosite	6.39×10^{-10}

tained by the creep analysis described in the previous section. Figure 3 shows the radial distribution of stresses in the solidified region in the case of granite, where t in the figure is the time after onset of heat extraction and the arrows are indicating the outer boundary of the solidified region at the respective time. The stress distribution is almost unchanged regardless of the growth of the solidified region with time, in contrast to

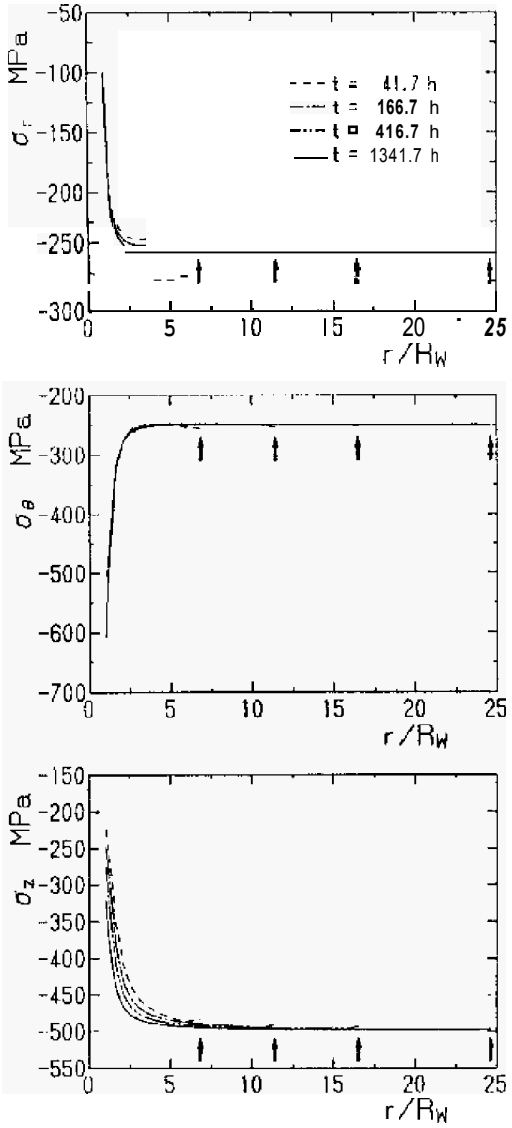

Figure 3. Stress distribution in the solidified region for granite (Arrows indicate the outer radius of the solidified region at each time).

stresses obtained by purely elastic analysis which change with time as shown in Figure 4 for comparison sake. In the case of anorthosite, stress distribution has an intermediate tendency between those of granite and the purely elastic case, as shown in Figure 5. Time variation of stresses on the inner boundary

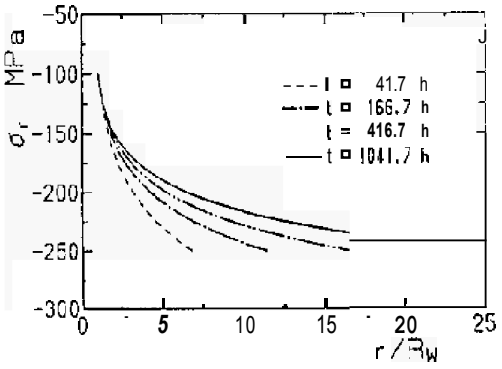

Figure 4. Stress distribution in the purely elastic case.

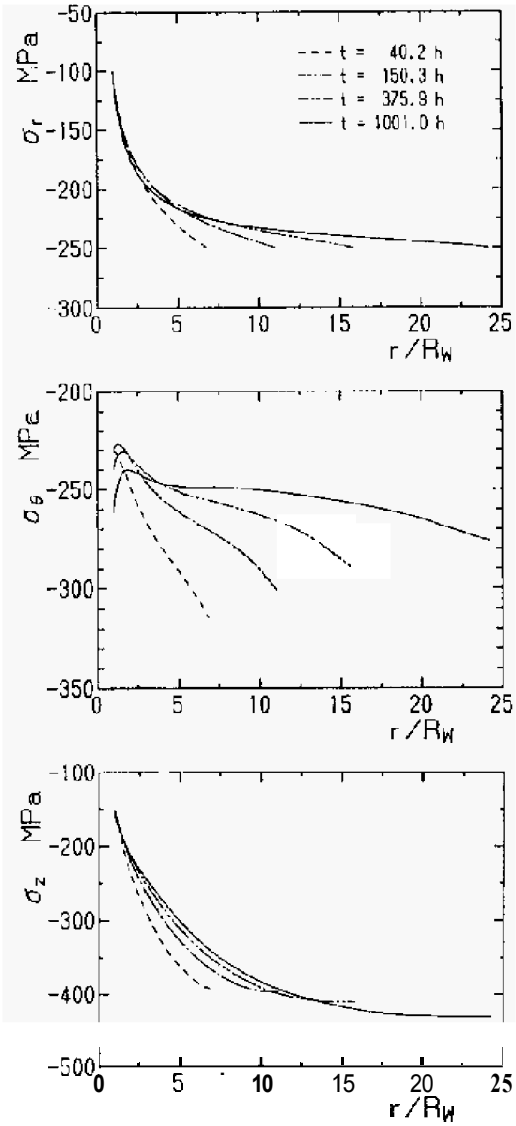

Figure 5. Same as Figure 3 for anorthosite.

of the solidified region is presented in Figure 6 and 7 for granite and anorthosite, respectively. In the both cases, the time variations are very moderate except for the very beginning of heat extraction, It is seen from Figures 6 and 7 that the stresses on the inner boundary are compressive for 10km deep even in the early stage of heat extraction. Although the results for the olivine are not presented here for brevity, stress distribution and its time variation are very similar to those of anorthosite.

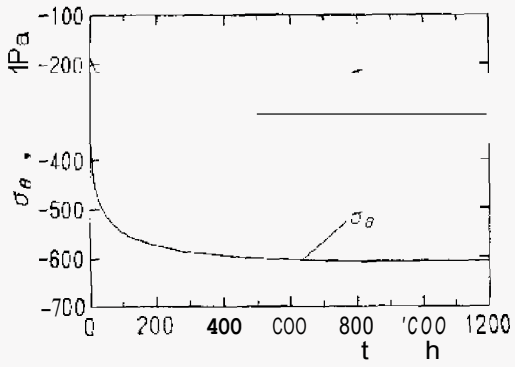

Figure 6. Time variation of circumferential and vertical normal stresses at the wellbore surface for granite.

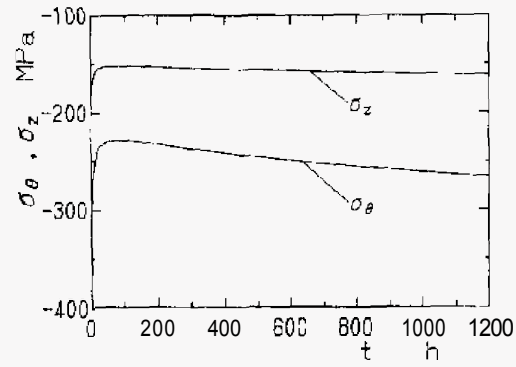

Figure 7. Same as Figure 6 for anorthosite

Olivine is most resistive to creep as stated before, but the temperature of solidus is highest. The effects of these two factors to creep deformation are opposite. This would be the reason why the two cases of olivine and anorthosite are similar to each other.

In the open system, formation of fractures and the extent of fractured region are crucial factors. In the following, let us discuss the variation of stress on the inner boundary of the solidified region with respect to the depth of the heat exchange system. In order to get the results for this purpose, the following boundary conditions are used: P_{in} = 40MPa and P_{out} = 100MPa for 4km deep, P_{in} = 60MPa and P_{out} = 150 MPa for 6km deep and P_{in} = 80MPa and P_{out} = 200MPa. Figures 8 and 9 show the

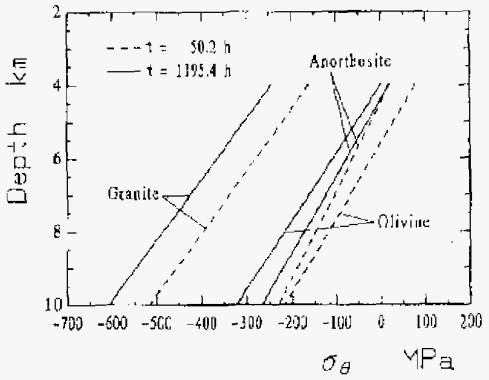

Figure 8. Variation of the circumferential normal stress on the well bore surface with respect to the depth of the heat exchange system.

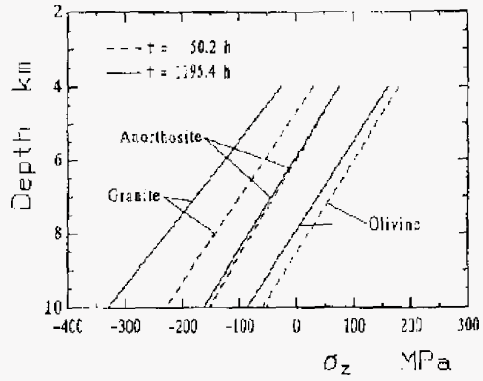

Figure 9. Same as Figure 8 for the vertical normal stress.

variation of stresses against the depth. In the case of granite, the circumferential stress σ_θ is always compressive and therefore radial fracture would hardly be formed. On the contrary, the circumferential stress for anorthosite and olivine has a tendency to be tensile in shallower depth. Regarding the normal stress, σ_z acting in the vertical direction it is also compressive for granite. However, it is tensile in the zone shallower than 8km for olivine and is also tensile in the zone shallower than 6km for anorthosite. Thus, it is highly probable that horizontal fractures are formed for olivine and anorthosite. In the case of granite, horizontal fractures are hardly formed, either. The results stated above imply that olivine would be the most potential candidate for direct extraction of magma energy and anorthosite comes next. Granite would not be appropriate.

REFERENCES

Bochm, R. F., Berg, Jr., D. L. and Ortega, A. (1989). Modeling of a Magma Energy Geothermal Open Cycle Power Plant. *Journal of Energy Resources Technology*, Vol.111, No.1, pp.239-245.

Chu, T. Y., Dunn, J. C., Finger, J. T., Roudle, J. B. and Westrich, H. R. (1990). The magma Energy Program, *Geothermal Resources Council Bulletine*, Vol.19, No.2, pp.42-52.

Colp, J. L. and Stoller, H. M. (1981). Utilization of Magma Energy-Project Summary. Energy Resources of the Pacific Region, *AAPG Studies in Geolgy* No.12, ed. Halbouty, M. T., The American Association of Petroleum Geologists, pp.541-551.

Colp, J. L. (1982). Final Report-Magma Energy Research Project, *Sand* 2 2377, Sandia National Laboratories, Albuquerque, NM.

Dunn, J. C., (1983). Energy Extraction from Crustal Magma Bodies, *ASME/JSME Thermal Engineering Joint Conference Proceeding*, Vol. II, pp.93-100.

Dunn, J. C., Ortega, A., Hicox, C. F., Chu, T. Y., Wemple, R. P. and Bochm, R. F. (1987). Magma Energy Extraction, *Transaction of 12th Workshop on Geothermal Reservoir Engineering*, Stanford University, CA, pp.13-20.

Dunn, J. C. (1989). Magma Energy Extraction-Annual Report for FY88, *Sand* 89-0567, Sandia National Laboratories, Albuquerque, NM.

Gerlach, T. M. (1981). Fuels from Magma-Potential Energy Resource? Energy Resources of the Pacific Region, *AAPG Studies in Geolgy* No.12, ed. Halbouty, M. T., The American Association of Petroleum Geologists, pp.553-536.

Hayashi, K. et al. (1991). Transient Hehavior of the Solidified Magma Region in the Direct Utilization of Magma Energy, *Journal of Geothermal Research Society of Japan*, Vol 13, No.4, pp.285-298, (in ,Japanese).

Hicox, C. E. and Dum, J. C. (1985). Preliminary Considerations for Extraction of Thermal Energy from Magma, *Geothermal Resources Council Transaction*, Vol.9, No.II, pp.319-324.

Kirby, S. H. end Kronenberg, A. K. (1987). Rheology of the Lithosphere: Selected Topics, *Geophysics*, Vol.25, No.6, pp.1219-1244.

Mendelson, A. (1968). *Plasticity, Theory and Application*, Macmillan.

Westrich, H. R., Weirick, L.J., Cygan, R. T., Reece, M., Hlava, P. F., Stockman, H. W. and Gerlach, T. M. (1986). FY1984 and FY1985 Geochemistry and Materials Studies in Support of the Magma Energy Extraction Program, Send 85-2843. Sandia National Laboratories, Albuquerque, NM.

Appendix

The temperature distributions were determined following the previous paper (Hayashi et al., 1991). Figures shown below are the temperature profiles for the several representative times after the onset of heat extraction, where the specific heat, the density, the latent heat, and the thermal conductivities of molten magma and solidified magma were set to be 1225J/kg/K, 2500kg/m^3, 2.72 x 10^{5}J/kg, 4.2W/m/K and 21W/m/K, respectively

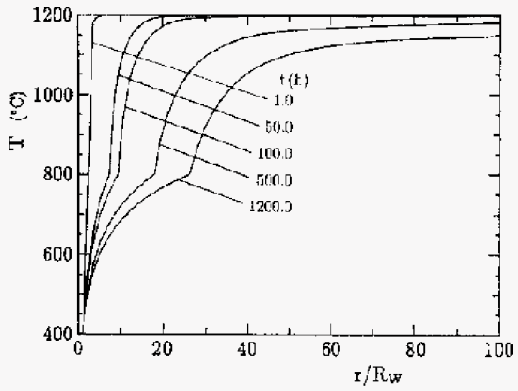

Figure A1. Temperature profiles for granite.

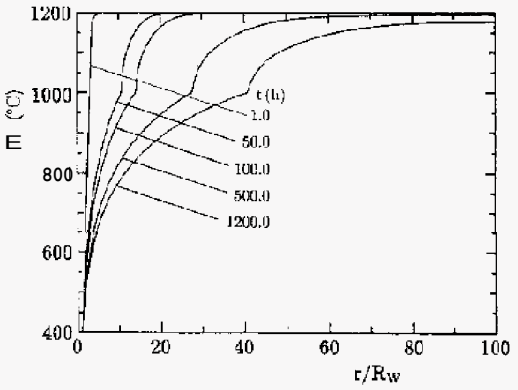

Figure A2. Temparature profiled for olivine.